Synthesis and Rheological Behavior of New Hydrophobically Modified Hydrogels with Tunable Properties

Guillaume Miquelard-Garnier, Sophie Demoures, Costantino Creton,* and Dominique Hourdet*

Physico-chimie des Polymères et des Milieux Dispersés, UMR 7615, UPMC−CNRS-ESPCI, 10 rue Vauquelin, 75005 Paris, France

Received June 19, 2006; Revised Manuscript Received August 28, 2006

ABSTRACT: New hydrophobically modified hydrogels have been designed in order to obtain a series of gels with identical elastic moduli but variable dissipative properties. The synthesis of these systems has been realized following a three-step procedure: (1) introduction of double bonds onto a poly(acrylic acid) backbone [PAA], (2) hydrophobic modification of the PAA with dodecylamine, and (3) cross-linking of double bonds using dithiol. The characterization of gel precursors shows that hydrophobically modified polymers self-assemble in semidilute solution forming physical gels with temporary hydrophobic clusters. The gelation mechanism induced by reacting pendant double bonds with dithiol was studied by DSC, specific titrations, and rheology. The gelation process was not perturbed by the presence of the hydrophobic groups, and the kinetics follows a first-order dependence on thiol. In the entangled regime, the thiol conversion reaches around 80%, but only about 10% of the thiols effectively promote the formation of chemical cross-links while the other 90% are incorporated into the gel as loops or dangling chains. Once the gels are formed, NMR and SANS clearly demonstrate that hydrophobic side chains continue to form micelles within the network and that these micelles display a much better long-range order than their un-cross-linked precursors in aqueous solutions. All gels, both hydrophilic and hydrophobically modified, display a storage modulus G' which only depends on total polymer concentration and can be described on the basis of the percolation theory ($G' \sim \epsilon^{2.6}$) with ϵ, the reduced concentration defined from a fixed concentration at the gel point $C_g = 2\%$. On the other hand, the loss modulus G'' increases dramatically relative to the corresponding hydrophilic gel, when hydrophobic groups which formed reversible associations are introduced.

Introduction

Polymer gels are broadly defined as polymer networks swollen to different degrees by a low molecular weight fluid. Typically, the entropy of mixing which causes the swelling is counterbalanced by the elastic deformation of the network which prevents dissolution, and the volume fraction of polymer in the gel and the degree of cross-linking of the polymer control its elastic modulus which is typically in the kPa range. A very common solvent used to swell polymer gels is water, and in this case the word hydrogel is often used. Hydrogels are particularly common in life sciences, food science, and various applications in engineering.[1,2] They are typically nontoxic and can be manufactured with a variety of different chemistries and with a wide range of elastic moduli.

Although a significant amount of literature is dedicated to the synthesis and swelling properties of hydrogels[3−7] and to the control of their elastic modulus,[8−11] much less attention has been paid to their mechanical strength,[12−14] i.e., resistance to fracture. Yet some gels have been reported as very tough and difficult to break,[15] while others (the majority) are quite brittle. The reasons for this tough or brittle behavior are poorly understood.

Some ideas can be inferred from the behavior of cross-linked polymer networks in the absence of solvent, i.e., the materials that are commonly called rubbers. Pure well-cross-linked rubbers are typically not very tough and fail at relatively low extensions, with the notable exception of natural rubber, which can crystallize under strain. However, when small filler particles, such as carbon black, are added to the rubbers, their fracture toughness increases significantly.[16,17] It is widely believed that this toughening mechanism is due to the existence of a percolating network of interactions between the particles that can break at large strains. This breakup of these interactions is a highly dissipative process, and since large strain is necessary at the tip of a crack before fracture, this makes it much costlier energetically to propagate a crack and fracture the rubber.

How can this concept of a percolating network of interactions be transferred to a much softer water-filled hydrogel? In general, hydrogels are very elastic materials which do not have many intrinsic mechanisms to dissipate energy during their deformation. It would however be interesting to obtain hydrogels where the elastic and the loss modulus could be independently controlled. Not only these gels would be promising candidates for better mechanical properties and resistance to fracture, but for some applications such as artificial tissue or cell spreading, it could be interesting to control not only the modulus of the scaffold or substrate but also its viscoelastic character.

Over the past 20 years, water-based formulations, and in particular associating water-soluble polymers, have received a lot of attention for both environmental and economic reasons.[18−22] These amphiphilic macromolecules contain a main hydrophilic part that maintains the solubility of polymer chains in water as well as hydrophobic moieties which provide the associative behavior. Once dissolved in water, these polymers self-assemble and form a transient network with hydrophobic clusters connecting hydrophilic chains.[23,24] These temporary associations of hydrophobic groups dramatically increase the viscosity of the solution[25] and have been modeled as polymers with sticker groups.[26]

However, their potential as building blocks for networks has not been evaluated. One possible method to create dissipative

* To whom correspondence should be addressed: e-mail costantino.creton@espci.fr, dominique.hourdet@espci.fr; Tel +33 (0)1 40 79 46 43; Fax +33 (0)1 40 79 46 86.

10.1021/ma061361n CCC: $33.50
Published on Web 10/20/2006

mechanisms and a breakable network of interactions in a hydrogel is precisely to introduce such hydrophobic interactions inside the gel. By chemically cross-linking water-soluble associating polymers,[27] a hydrogel with both permanent and reversible junctions can be formed.[28,29] The hydrophobic clusters with a characteristic lifetime are expected to induce dissipative mechanisms in the hydrogel, so that its mechanical properties and especially loss modulus and hysteresis should be increased. By analogy with the behavior of rubbers, we can expect also an improved fracture resistance for the same elastic modulus.

We present in this paper a possible route to such materials with the synthesis and mechanical characterization of new hydrogels which have been chemically modified to have hydrophobic short chains along their backbone.

The main goal of our study is to understand the role of temporary cross-links in the fracture mechanism of hydrogels. In this first article, we focused on a new way of synthesizing hydrophobically modified hydrogels starting from self-assembling properties of poly(sodium acrylate) grafted with alkyl groups and using the reactive properties of thiols for chemical cross-linking. The rheological behavior of these systems is also reported, and we show that the properties of these new hydrogels can be easily controlled on the basis of the polymer concentration, the amount of hydrophobic groups introduced, and the quantity of cross-linker and/or initiator.

Experimental Part

Reactive and Solvents. Dithioerythritol ($C_4H_{10}O_2S_2$), diallylamine (C_3H_7N), and dodecylamine ($C_{12}H_{27}N$) were purchased from Aldrich and were used without further purification. Potassium peroxodisulfate (Prolabo), dicyclohexylcarbodiimide (DCCI, from Acros Organics), and *N*-methylpyrrolidone (NMP, from SDS) were all analytical grade reagents. Water was purified with a Millipore system.

Materials. The syntheses of modified polymers and hydrogels can be summarized as follows:

Polymer Precursor. Poly(acrylic acid) (PAA) was obtained in its acid form as a 35 wt % solution in water from Aldrich. The solution was diluted to 10 wt % and freeze-dried. Its number-average molecular weight as characterized by size exclusion chromatography (SEC) was $M_n = 35$ kg/mol ($I_P \sim 10$). This molar mass falls in an intermediate range: not too low to favor interchain cross-linking but not too high to prevent entanglements at low concentrations.

Modification of PAA. PAA chains were submitted to different chemical modifications. All the polymer chains were initially modifed by introducing a given proportion of double bonds (allylamine) along the backbone to cross-link the chains afterward, while some of them were also submitted to additional modification with different proportions of short hydrophobic chains (dodecylamine). Both reactions were carried out by grafting amino-terminated molecules (allylamine and dodecylamine) onto the carboxylic acids of the polyacrylic backbone in the presence of dicyclohexylcarbodiimide (DCCI) which activate the formation of the amide bound (see Figure 1).[30]

The grafting procedure used for both allylamine and dodecylamine can be summarized as follows: In a three-necked flask equipped with a reflux condenser and a magnetic stirrer, 10 g of poly(acrylic acid) precursor was initially dissolved in 200 mL of NMP for 12 h at 60 °C. Separately, the amino compound (allylamine or dodecylamine) and DCCI were dissolved in a small volume of NMP. The solution of amine was then slowly added into the reaction medium followed by a dropwise addition of DCCI. The reaction was allowed to proceed at 60 °C. After 24 h, the solution was cooled to room temperature, and dicyclohexylurea was eliminated by filtration. The modified PAA was then precipitated with a dropwise addition of a concentrated solution of sodium hydroxide ([NaOH]/[COOH] ≅ 4). It was recovered by filtration

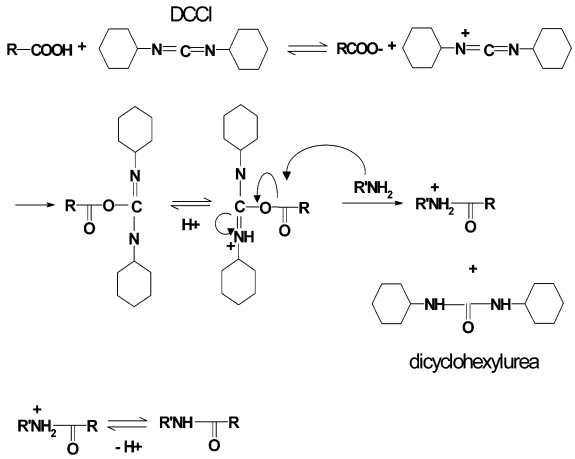

Figure 1. General mechanism for the condensation between carboxylic acid and amine in the presence of carbodiimide.

and washed several times with methanol prior to drying under vacuum overnight at room temperature. The modified polymer was then dissolved in water ($C \sim 5\%$ w/w) and dialyzed for 1 week against pure water (membrane cutoff = 3.5−5 kg/mol) in order to remove low molecular weight impurities (methanol, NMP, NaOH) and to lower the pH below 8, as thiols used for cross-linking have a typical pK_a between 10 and 12. The solution was finally freeze-dried, and the dry modified PAA was recovered in its sodium salt form. Three different polymers were synthesized with 10 mol % double bonds and various molar amounts of C12: 0, 3, and 5%. These three polymers are called PAA10db, PAA3C12, and PAA5C12, respectively.

Chemically Cross-Linked Hydrogels. The choice of the cross-linking route was mainly motivated by the constraint to carry out the synthesis in water because we wanted to avoid any exchange of solvent for some of our mechanical tests. Thiols can easily produce radicals by a redox mechanism with potassium peroxodisulfate. These radicals are very reactive with the double bonds,[31−34] and a network can be readily formed if multifunctional thiols are used, like dithioerythritol. As described in the following, the reaction was carried out in water, at room temperature, and under atmospheric conditions, i.e., in the presence of oxygen which does not inhibit the reaction.[31] Modified PAA, dithioerythritol, and KPS were separately dissolved in water at the desired concentration. All concentrations, for solutions and gels, are expressed in % w/w.

PAA and KPS are dissolved 12 h before the gel reaction to allow good homogeneity of the solutions.

The KPS was then added to the PAA solution under stirring, and finally dithioerythritol was quickly added into the solution. Since dithioerythritol is known to react with itself and to form disulfur linkages, solutions were always freshly prepared before mixing. After an energetic stirring during a few seconds, the solution was finally left to rest for gelation.

Characterization. *Titration Methods of Functional Groups in the Hydrogel*. To estimate the yield of the cross-linking reaction, we developed a series of titration methods. S−H functions can be reduced by I_2 under acidic conditions[35] following the redox reaction:

$$2RSH + I_2 \rightarrow RSSR + 2H^+ + 2I^-$$

I_2 can also react with the free double bonds of the network, following the electrophilic addition reaction:

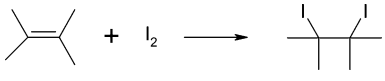

The iodide titration method was first separately tested for these two functions with a solution of modified PAA and with a solution of thiol and was found to be quantitative in both cases.

Table 1. Nomenclature and Composition of Modified PAA[a]

	grafting ratio (mol %)			grafting yield (%)			
polymers	DB	C12	$N_{C12/chain}$	DB	C12	reaction yield (%)	M_{eq} (kg/mol)
PAA							0.094
PAA10db	10	0	0	100	100	80	0.0957
PAA3C12	10	3	11	100	100	50	0.1
PAA5C12	10	5	19	100	100	50	0.1027

[a] $N_{C12/chain}$ is the average number of grafts per PAA chain, and M_{eq} is the average molar mass per monomer unit of the main chain, with the PAA under Na salt form.

To separate the thiols from the double bonds, the S−H functions were specifically titrated with Fe^{3+}, following the redox reaction:

$$2RSH + 2Fe^{3+} \rightarrow RSSR + 2H^{+} + 2Fe^{2+}$$

The following protocol was used: 1 mL of gel was prepared in a test tube by mixing a given amount of polymer precursor with an equimolar concentration of double bonds, −SH and KPS. The solution of PAA modified with double bonds, and the solution of thiols was titrated with I_2 before mixing in order to determine the initial quantity of each component. After 3 h of reaction, 1 mL of HCl at 1 mol/L was added. The protonation of the carboxylic functions prevented the hydrogel from high swelling. From this stage, several analyses were carried out: (1) 100 mL of I_2 at 10^{-3} mol/L was added to the gel, and the reaction was left for 36 h in order to homogenize the system. Finally, the excess of I_2 was titrated with a solution of sodium thiosulfate at 10^{-3} mol/L. (2) In another similar test tube, 100 mL of an $FeCl_3$ solution at 10^{-3} mol/L was added to the protonated gel. After 36 h, the Fe^{2+} ions, formed according to the redox reaction, were titrated with a solution of $KMnO_4$ (10^{-4} mol/L) following a potentiometric method. (3) After acidic treatment of the hydrogel, solutes and unreacted molecules were extracted with 25 mL of water for 4 h. This extraction was repeated four times. The washing solutions were collected and titrated with I_2 in order to determine the concentration of free thiols extracted from the gel.

Rheology. Steady-state viscosity of aqueous solutions of network precursors was measured in the linear regime with a Contraves LS 30 low shear rheometer.

Rheological properties of the hydrogels in oscillatory shear were carried out with a stress-controlled rheometer TA Instruments AR 1000 using a cone−plate geometry with a radius of 4 cm, a truncature of 55.9 μm, and a small angle of 2°. The reproducibility was verified for each experiment.

Several rheological analyses were carried out in order to investigate the effect of polymer concentration and hydrophobic modification on gelation kinetics and viscoelastic properties of the resulting gels. All the polymer concentrations are given in % (w/w).

Differential Scanning Calorimetry. The cross-linking reaction was followed by differential scanning calorimetry (DSC) with a microDSC III from Setaram using a mixing cell divided in two compartments. One was filled with the solution of PAA and KPS, while the other was filled with the thiol solution. At $t = 0$, the trap between the two compartments was opened and a rapid mixing took place. Hydrogels were equilibrated with a reference mixing cell, filled with the same quantity of polymer, cross-linker, and solvent but without KPS, and the heat flow of the reaction was followed as a function of time. The mixing contribution (exothermic process), observed at the very beginning of the reaction, was also measured independently using the mixing cell. In that case, the first compartment was filled with a solution of PAA and KPS, while the other was filled with water without cross-linker so that no reaction occurred during the mixing process. The reference was there only filled with water. This mixing enthalpy was found to be negligible compared to the heat of the reaction.

Small-Angle Neutron Scattering (SANS). SANS experiments were performed at Laboratoire Léon Brillouin, Saclay, France. The experiment was carried out at $T = 20$ °C, using an incident neutron beam of wavelength $\lambda = 12$ Å with a corresponding sample-to-detector distance of 1.7 m. Samples were initially prepared by dissolving polymers in D_2O as solvent with or without cross-linker (dithioerythritol and KPS). The solutions were then quickly transferred into 5 mm thick quartz containers for SANS experiments. For reactive media, the cross-linking reaction was left to proceed for at least 24 h before the SANS experiments. The coherent scattering intensity of the samples was obtained by subtracting the background signal given by the pure D_2O sample. The efficiency of the detector cell was normalized by the intensity delivered by a pure water cell of 1 mm thickness. Absolute measurements of the scattering intensity $I(q)$ (cm^{-1} or 10^{-8} $Å^{-1}$) were obtained from the direct determination of the incident neutron beam flow and the cell solid angle.[36]

NMR. ^1H and ^{13}C NMR were carried out using an Avance Brücker spectometer at respective frequencies of 300 and 75.48 MHz. All the experiments were performed in D_2O.

Results

Solutions: Structure and Behavior of Modified PAA. a. Polymer Structure. The gel precursors PAA10db, PAA3C12, and PAA5C12 were characterized by ^1H NMR in D_2O. After identification and integration of the peaks for each polymer, as shown in Figure 2a,b, the average composition of the polymers was determined (see Table 1).

The ^1H NMR data show that the grafting reaction is quantitative and well controlled for both types of modification, allylamine and amino-C12. Since the reaction medium is fully homogeneous (PAA, allylamine, and C12 are readily soluble in NMP) and the molecular weight of the PAA precursor is high enough, we will consider that both double bonds and hydrophobic tails are randomly distributed along the backbone. For instance, the existence of such a distribution was clearly proved with C12 derivatives of PAA by Iliopoulos and co-workers using larger amounts of C12.[30]

PAA10db, which does not contain hydrophobic groups, was also characterized by SEC, and the molar mass distribution remained unchanged relative to that of the PAA precursor.

If the grafting reaction is quantitative, whatever are the substituents, the reaction yield is lower in the case of hydrophobically modified PAA. This is attributed to the higher affinity of dodecyl chains in organic solvents, which renders the precipitation step more difficult.

b. Viscosity of the Polymer Solutions. Unlike nonionic macromolecular coils, polyelectrolyte rods start to overlap at extremely low concentrations (C^*). Consequently, the semidilute regime generally spans down to very low concentrations, and the transition between dilute and semidilute regimes is often out of range of applications. Moreover, C^* cannot be easily determined by rheology since the viscosity of polyelectrolyte solutions, at low ionic strength, follows the same Fuoss law ($\eta \sim C^{1/2}$) in both dilute and semidilute unentangled regimes. It is only above the entanglement concentration (C_e) that the viscosity starts to increase with a higher exponent ($\eta \sim C^{3/2}$) as theoretically described by Dobrynin et al.[25] In the present case, if we use the theoretical relations proposed by Dobrynin et al.[25] we can roughly estimate a critical overlap concentration of PAA

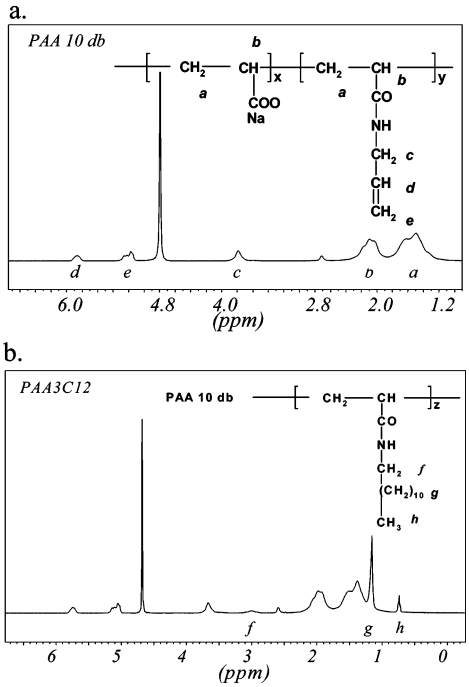

Figure 2. ^{1}H NMR spectra (300 MHz) and assignments for solutions of PAA10db and PAA 3C12 in D_2O. The peak at 4.8 ppm is assigned to HOD.

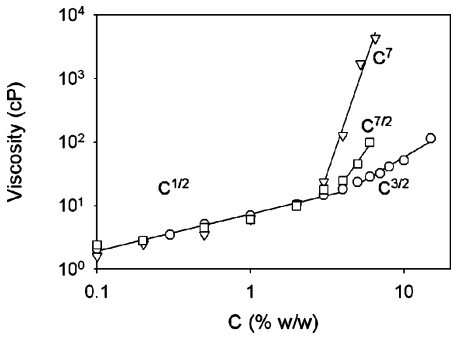

Figure 3. Variation of the viscosity with the concentration for aqueous solutions of PAA10db (●), PAA3C12 (■), and PAA5C12 (▼).

chains around $C^* \sim 2 \times 10^{-2}$ %, i.e., well below the range of concentrations investigated.

As shown in Figure 3, the viscosity of the hydrophilic precursor PAA10db in aqueous solution is in good agreement with the theoretical predictions; exponents 0.56 and 1.62 were found for unentangled and entangled regimes, respectively. This gives a rough estimate for the beginning of the entangled regime, which occurs around $C_e = 5-6\%$.

Below $C = 2\%$, the solutions of hydrophobically modified polymers (PAAxC12) have a slightly lower viscosity compared to that of the hydrophilic precursor. In this concentration range, hydrophobic associations mainly occur intramolecularly and tend to reduce the hydrodynamic radius of the macromolecules.[29] Nevertheless, at low ionic strength the collapse of the chain induced by the hydrophobic aggregation is generally not very high due to the strong electrostatic repulsions which dominate the conformational behavior. On the contrary, above 3% for the PAA5C12 and above 4% for the PAA3C12, the viscosity of hydrophobically modified polymers increases sharply with a much higher scaling coefficient ($\eta \sim C^7$ and $\eta \sim C^{7/2}$, respectively). The viscosity of these associating polymers becomes rapidly several orders of magnitude higher than that of the PAA precursor in the entangled regime. Such a high value of the scaling coefficient is expected in this concentration regime

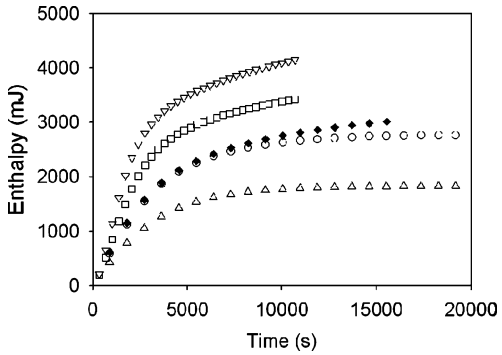

Figure 4. Variation with time of the enthalpy of the thiol−ene reaction performed between modified PAA and dithioerythritol in stoichiometric conditions. Experimental results were obtained for PAA10db at 10% (▽), 8% (□), 6% (○), 5% (△), and PAA3C12 at 6% (◆).

as long as the concentration remains below the overlap concentration of the strands between the associating stickers. It mainly corresponds to the transformation of intramolecular bonds into intermolecular ones.[37]

Sol−Gel Transition. a. Kinetics of the Cross-Linking Reaction. The cross-linking reaction was followed by micro-DSC experiments at $T = 25$ °C where the heat flow due to the reaction was analyzed as a function of time. The integration of the heat flow gives the reaction enthalpy vs time as shown in Figure 4. The cross-linking reaction involves a radical addition of a thyil group onto a vinyl functional group (step 1), followed by radical transfer from the ensuing carbon radical to a thiol functional group (step 2). If the second thiol of the bifunctional mercaptan reacts with a vinyl from another PAA chain following steps 1 and 2, a cross-link is formed (step 3).

$$HS-RS^{\bullet} + R'CH{=}CH_2 \rightarrow R'C^{\bullet}H-CH_2SR-SH \qquad \text{(step 1)}$$

$$R'C^{\bullet}H-CH_2SR-SH + RSH \rightarrow R'CH_2-CH_2SR-SH + RS^{\bullet} \qquad \text{(step 2)}$$

$$R'CH_2-CH_2SR-S^{\bullet} + R''CH{=}CH_2 \rightarrow \rightarrow R'CH_2-CH_2SR-SCH_2-CH_2R'' \qquad \text{(step 3)}$$

Interestingly, no significant differences (less than 10%, which is within the reproducibility of the measurements) were observed with DSC between modified and unmodified hydrogels prepared at the same concentration. This seems to demonstrate that the kinetics of the cross-linking reaction is not much influenced by the presence of hydrophobic clusters. For similar thiol−ene reactions, Cramer et al.[38] have shown that the transfer (step 2) was the rate-limiting step of the reaction. From a large set of experimental data, they have modeled the kinetics of the reaction by considering that the rate constant of propagation (k_p in step 1) was much higher than the rate constant of the chain transfer process (k_{CT} in step 2); typically, $k_p/k_{CT} = 10$. In that case, the reaction rate (R) is first-order overall, with a first-order dependence on thiol functional group concentration and independent of the ene concentration:

$$R = k[SH]^1[C{=}C]^0 \qquad (1)$$

If we use a similar kinetics scheme for our reactions, taking into account that we are always in the same stoichiometric conditions, and if we assume that the consumption of thiols in the initiation process is low and negligible compared to the propagation, we can write that

$$R = -\frac{\mathrm{d[SH]}}{\mathrm{d}t} = k[\mathrm{SH}] \quad (2)$$

After integration of eq 2 it is possible to describe the conversion of SH functions (p) as a function of time:

$$p = \frac{[\mathrm{SH}]_0 - [\mathrm{SH}]}{[\mathrm{SH}]_0} = 1 - \exp(-kt) \quad (3)$$

with [SH] and $[SH]_0$ the thiol functional group concentrations at time t and at the beginning of the reaction.

As described previously, the reaction is followed by calorimetry and the conversion with time can be related to the enthalpy of the thiol−ene reaction:

$$p = \frac{\Delta H_t}{\Delta H_{100}} \quad (4)$$

where ΔH_t and ΔH_{100} are the variations of the reaction enthalpy at time t and at full conversion of SH groups.

Using eqs 3 and 4, it comes that

$$\Delta H_t = \Delta H_{100}(1 - \exp(-kt)) \quad (5)$$

Nevertheless, as it will be discussed in the next section, the reaction of the SH functions is not fully quantitative for all the reactions. A high and constant conversion ($p_{\mathrm{plateau}} = 0.8$) is obtained for all the systems prepared in the entangled regime ($C \geq 6\%$) while a lower conversion is obtained below C_e ($p_{\mathrm{plateau}} = 0.55$ for $C = 5\%$). This can be taken into account by replacing in the previous equation ΔH_{100} by $\Delta H_{\mathrm{plateau}}$, the reaction enthalpy at very long time that we will identify as the end of the experiment:

$$\Delta H_t = \Delta H_{\mathrm{plateau}}(1 - \exp(-kt)) \quad (6)$$

The calorimetric data are plotted in Figure 5 according to eq 6, and we can see that the results agree fairly well with this kinetics scheme assuming a first-order reaction with respect to SH functions. For all the experiments a plateau is reached at $\Delta H_{\mathrm{plateau}} = 270 \pm 30$ kJ/mol SH. The differences are within the range of experimental errors assuming 5−10% on DSC experiments and 10% on titration techniques which have been used to estimate the conversion. Similarly, eq 6 is able to fit nicely the experimental data with a rate constant $k = (3 \pm 0.4) \times 10^{-4}$ s^{-1}. This value corresponds to a characteristic time $\tau = k^{-1} \cong 3300$ s for all the reactions, independently of the concentration, and to a total reaction time $t \sim 15000-20000$ s assuming a limited conversion of SH groups ($p = 0.8$).

b. Kinetics of Gelation. Compared to DSC which provides information at the molecular level of the thiol−ene reaction, it is interesting to analyze by rheology the modifications involved at the macroscopic level during this reaction: the so-called gelation process. After addition of KPS and dithioerythritol in the PAA solution, followed by a rapid stirring, the liquid solution (sol) is introduced in the rheometer, and the dynamic moduli were measured as a function of time in isothermal conditions, $T = 25$ °C. If not specified, all the rheological measurements presented in the following were performed in the linear regime (1% strain) and at a constant frequency of 1 Hz. The experiments were carried out in water between 2 and 10% for hydrophilic polymers (PAA10db) and at lower concentrations ($C = 2-7\%$) for hydrophobically modified systems. For PAA5C12 for instance, it was not possible to investigate concentrations above 6% as the high level of viscosity caused a very poor and inhomogeneous mixing of the solution.

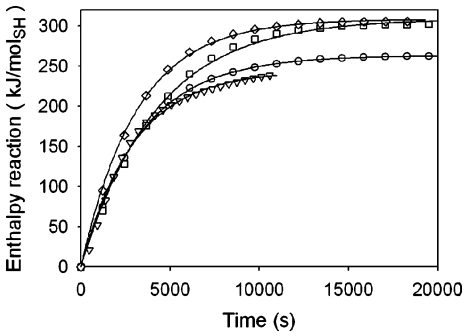

Figure 5. Enthalpy reaction for a mole of reactive thiol as a function of time for several hydrogels: PAA 5% (◇), PAA3C12 5% (□), PAA3C12 6% (○), PAA 8% (▽). Fits are represented by the straight lines.

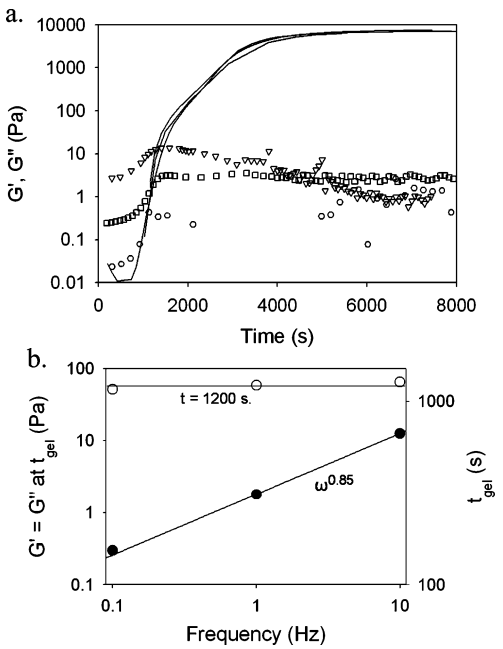

Figure 6. Sol−gel transition of an aqueous solution of PAA10db ($C = 8\%$ w/w) followed at 0.1 Hz (○), 1 Hz (□), and 10 Hz (▽). (a) For clarity, G' was represented with a straight line for the three frequencies. (b) Left axis: $G'(t_{\mathrm{gel}}) = G''(t_{\mathrm{gel}})$ as a function of frequency (black circles). Right axis: t_{gel} vs frequency (open circles).

Gelation of PAA10db. As shown in Figure 6, a sol−gel transition is clearly observed for the hydrophilic PAA10db system with a strong upturn of the elastic modulus (G') which becomes higher than the loss modulus (G'') after ∼1200 s.

This crossover of G' and G'' is almost independent of the frequency of measurement for at least 2 decades, and we will use this peculiarity to define the gel point as proposed by Winter and Chambon.[39−41] While the gel time (t_{gel}) is frequency independent, G' and G'' increase at the gel point and follow a similar dependence with the frequency, i.e., $G'(t_{\mathrm{gel}}) = G''(t_{\mathrm{gel}}) \sim \omega^n$ in agreement with the description of Winter and Chambon. The scaling exponent n is generally equal to $^1/_2$ if there is a balanced stoichiometry between polymer and cross-linker, lower than $^1/_2$ if the cross-linker is in excess, and higher to $^1/_2$ in the opposite case. For our unmodified PAA hydrogels, the exponent was found equal to 0.85, which would imply a slight under stoichiometry concentration of thiols compared to double bonds.

Of course, the concentration is a key parameter for gelation, and we can observe in Figure 7 that t_{gel} decreases exponentially with polymer concentration. For $C = 2\%$, the gelation almost

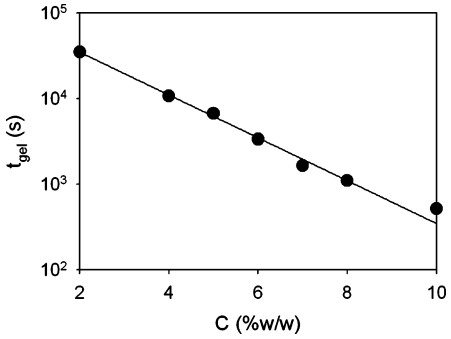

Figure 7. t_{gel} as a function of concentration for unmodified hydrogels.

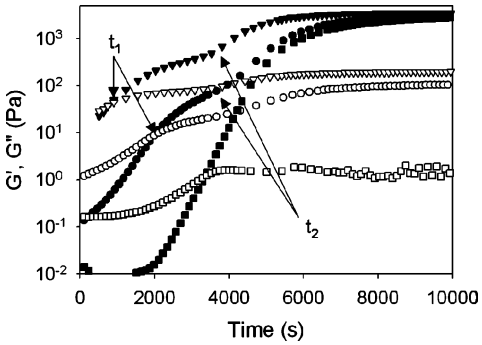

Figure 8. Comparison of the gelation process for aqueous solutions ($C = 6\%$) of PAA10db (■, G'; □, G''), PAA3C12 (●, G'; ○, G''), and PAA5C12 (▼, G'; ▽, G''). $f = 1$ Hz.

does not occur, as a very long time is needed ($t_{gel} = 35000$ s) to get the crossover of dynamic moduli. In that case, G' and G'' remain very weak (0.5 Pa), and we will define this concentration as the critical gel concentration of the system (C_{gel}).

Gelation of Hydrophobically Modified Hydrogels. For comparison, the sol−gel transition of various hydrophobically modified polymers studied at the same concentration is reported in Figure 8.

Several interesting observations can be made. First of all, if we analyze the plateau values of the moduli, we can see that the loss modulus of hydrophobically modified hydrogels is significantly higher than the loss modulus of the hydrophilic one while the storage modulus is insensitive to the presence of hydrophobic groups. This remarkable result, which will be discussed in more detail in the section dedicated to the mechanical characterization of hydrogels, implies that the presence of hydrophobic groups in the network adds a dissipative character which did not exist without them. If we look at now the kinetics of the sol−gel transition, we observe that the crossover of dynamic moduli is clearly shifted toward lower times with increasing hydrophobic content. This indicates that the presence of alkyl groups renders the material more solidlike much sooner. However, there is a second inflection point for the hydrophobically modified systems, for both G' and G''. This second transition occurs at times that are very close to the "gelation" threshold determined for the hydrophilic sample (t_2 in Figure 8). If we define t_2 as the inflection point of the increasing rates of G' and G'' vs time, we get $t_2 \sim 3500$ s for the PAA3C12 system ($C = 6\%$), which is equal to t_{gel} determined for PAA10db at the same concentration. Some additional experiments were performed to clarify the two-step gelation process evidenced for hydrophobically modified hydrogels. For example, the first transition (t_1) is not observed at low polymer concentration for PAA3C12 ($C = 4\%$, see Figure 9) or PAA5C12 ($C = 3\%$).

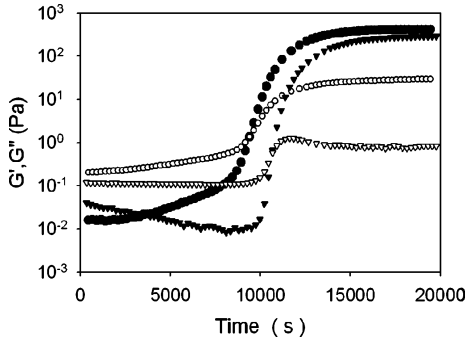

Figure 9. Comparison of the gelation process for aqueous solutions ($C = 4\%$) of PAA10db (●, G'; ○, G'') and PAA3C12 (▼, G'; ▽, G''). $f = 1$ Hz.

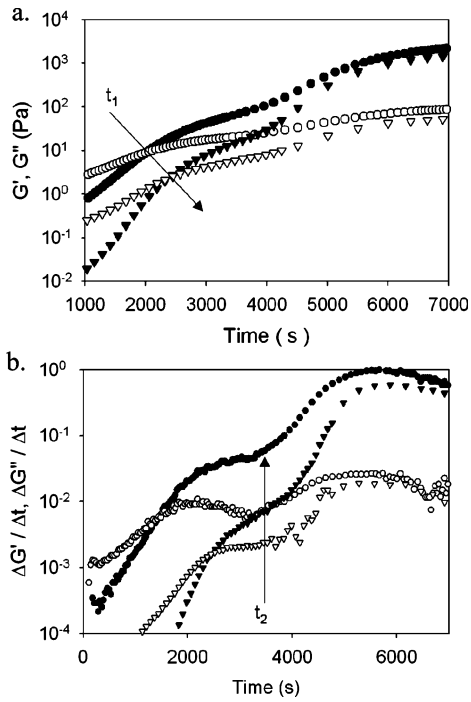

Figure 10. Comparison of the gelation process for aqueous solutions of PAA3C12 ($C = 6\%$) at different frequencies 1 Hz (●, G'; ○, G'') and 0.1 Hz (▼, G'; ▽, G''): (a) dynamic moduli vs reaction time and (b) their derivatives.

Moreover, if the gelation is followed at different probing frequencies, as shown in Figure 10, t_1 is found to be very frequency dependent while t_2 is not. We can even imagine that t_1 would not appear at all at high frequency. Since t_1 depends on the frequency of measurement, on the polymer concentration, and on the concentration of hydrophobic groups in the gel (these two parameters being related), we can conclude that it is sensitive to the dissipative effects induced by the associations between hydrophobic groups, while t_2 reflects the chemical reaction and in consequence is independent of these parameters.

Structure and Behavior of Hydrophobically Modified Hydrogels. The stated goal of this work was to synthesize and characterize well-controlled hydrogels containing both chemical cross-links and hydrophobic intermolecular associations. In the previous section we have shown that such hydrophobic associations occur in aqueous solution. We will now characterize the structure and the properties of chemically cross-linked hydrogels in order to study hydrophobic associations in the covalent network and how they affect the viscoelastic properties of the final hydrogel.

Self-Assembling Properties in Solution and Covalent Network. *^{13}C NMR.* Although ^{1}H NMR does not provide any

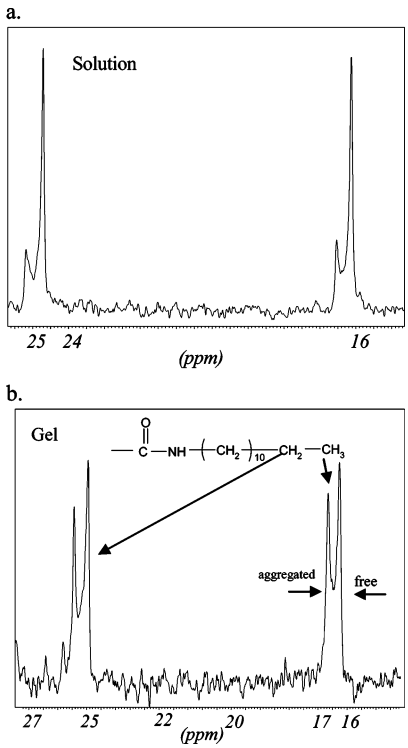

Figure 11. ^{13}C NMR spectra of PAA5C12 solution (a) and gel (b) in D_2O ($C = 4\%$). Peak splitting observed for terminal group (around 16 ppm) and vicinal methylene carbon (around 25 ppm) correspond to the free and aggregated form at high field and low field, respectively.

Table 2. Degree of Clustering of Dodecyl Groups in Gel and Solution State

		PAA3C12		PAA5C12	
		clustered (%)	free (%)	clustered (%)	free (%)
4% w/w	solution	0	100	20	80
	gel	10	90	40	60
5% w/w	solution	10	90	35	65
	gel	25	75	50	50

further information about the gel structure because of the broadening of the peaks due to the gelation, it is possible to use ^{13}C NMR to investigate the degree of clustering of alkyl groups either in solution or in the gel state. Indeed, the chemical shifts of the carbon nuclei of the alkyl groups depend on their chemical environment, which changes whether the hydrophobic tail is free (polar aqueous environment) or clustered within micelles (low-polarity environment). If the exchange is slow compared to the NMR characteristic time scale, a clear peak splitting is observed corresponding to free and clustered forms. This has been well described by Petit et al.[42] with aqueous solutions of PAA modified by alkyl or perfluoroalkyl side chains.

The ^{13}C NMR spectrum of the PAA5C12 gel at 4% is given in Figure 11. The peak splitting corresponding to the terminal methyl group (~16 ppm) and to the vicinal methylene carbon (~25 ppm) is clearly observed. By integrating the signals, we can estimate that about 20% of C12 are clustered in solution and 40% in the gel state. This proportion varies with concentration of polymer and hydrophobic groups, as reported in Table 2.

As already observed by Petit et al.,[42] we can see that the fraction of alkyl groups involved in the aggregation process increases with polymer concentration, whatever the system is, solution or gel. Similarly, we observe a significant increase of the clustering after gelation. In other words, it appears that the formation of covalent bonds significantly modifies the structure of the transient network. The introduction of covalent bonds shifts the initial competition between attractions (hydrophobic aggregation) and repulsions (electrostatic repulsions) in favor of hydrophobic interactions.

Table 3. Swelling Experiments on 6% w/w Hydrogels

	PAA10db	PAA3C12	PAA5C12
$m_{polymer}$ (g)	0.0246	0.0252	0.0216
$m_{gel-C\ preparation}$ (g)	0.42	0.41	0.36
$m_{gel-equilibrium\ swelling}$ (g)	2.1	2	1.9
Q_e	85	80	88

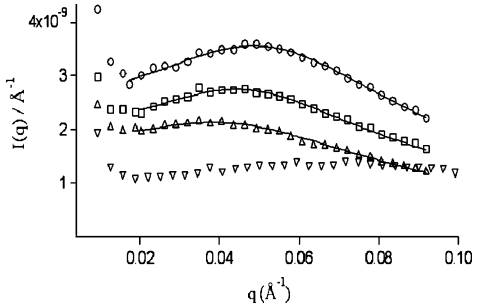

Figure 12. Scattering profiles of PAA5C12 hydrogels and solutions in D_2O at various concentration (6%, ○; 5%, □; 4%, △; 6% solution, ▽), with the fitting curves.

We also performed some swelling experiments to study the aggregation process at the equilibrium swelling. Hydrogels at 6 wt % polymer were put in an excess of pure water for 2 days, until the equilibrium swelling was reached, and the swelling ratio was determined by weighing. The results are reported in Table 3. These results clearly show that the presence of hydrophobic groups in the gel do not affect the swelling at equilibrium, i.e., at low polymer concentrations. This result is in agreement with data previously reported for similar systems,[43] showing that at low concentration electrostatic repulsions dominate hydrophobic interactions.

Small-Angle Neutron Scattering. The local structure of hydrophobic clusters was also investigated by small-angle neutron scattering in the case of PAA5C12 solutions and gels in D_2O (the 3C12 polymer did not give enough intensity to be studied properly).

The scattering spectra reported in Figure 12 clearly display the existence of an organized structure in aqueous medium, especially for gels. For instance, all the curves are characterized by a correlation peak which arise from the formation of interacting hydrophobic cores. The position of the correlation peak (q_{max}) is shifted to higher q values (or smaller distances) with increasing concentration of polymer and consequently increasing concentration of hydrophobic domains.

The scattering profiles also confirm that the micelles in the gel state are much better organized than in the solution state, as the scattering peak intensity is strongly enhanced after gelation. A more detailed analysis of these scattering patterns was carried out using a simple micellar model.[44] In this model we considered spherical polydisperse micelles of C12 with an average radius R_m and a Gaussian size distribution $\omega(r)$. These micelles, surrounded by PAANa chains making bridges and loops around the cores, interact with each other with a hard-sphere potential of average radius R_{HS} (see Figure 13).

The hypotheses that are made on the form factor (spherical objects) and the structure factor (repulsion with a hard-sphere potential) were described elsewhere.[45] The model was applied to our results using an absolute fitting of the data on the 5C12 system in solution and gel state. As we assume a dry core for

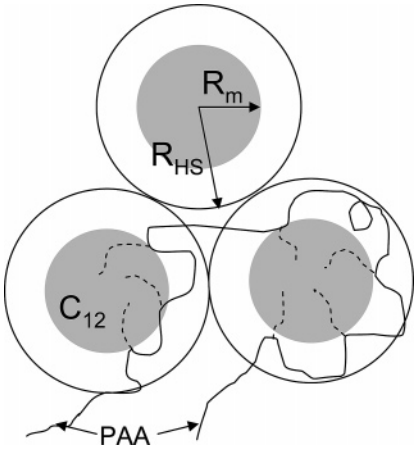

Figure 13. Schematic description of the micellar model with hard-sphere interactions used to describe self-assembling of grafted PAA in hydrophobically modified hydrogels.

Table 4. Fitting Parameters Obtained from SANS Performed on PAA5C12/D_2O Gels and Solutions at $T = 20$ °C

concentration	q_{max} (Å^{-1})	f_{C12} (%)	R_m (Å)	σ (Å)	R_{HS} (Å)
4% (gel)	0.044	37	18.3	1.9	45.8
5% (gel)	0.049	51	18	0.9	46.4
6% (gel)	0.053	71	17.8	1.2	42.3
6% (sol)	0.053	57	14	2.5	35

hydrophobic micelles, the model involves three parameters which are R_m, R_{HS}, and f_{C12}, the fraction of C12 which participate to the aggregation. The polydispersity with standard deviation σ is mainly used to improve the fit but does not influence much the choice of the previous parameters.

The fitting results are reported in Table 4. For all gel concentrations, this model appears to describe fairly well the experimental data (see Figure 12), supporting the picture of repulsive hydrophobic micelles. The model gives an average dry core radius $R_m \sim 18$ Å of low polydispersity ($\sigma \sim 1-2$ Å), which is in good agreement with the geometric distance calculated between the first and the last carbon of the C12 side chain in a planar zigzag conformation (~15 Å). Because of the presence of the polyelectrolyte shell, the hydrophobic cores are repulsive at short distances, and these interactions are simply described in this model by a hard-sphere potential ($R_{HS} = 42-46$ Å). The decrease of the hard-sphere radius with increasing polymer concentration can be ascribed to the self-screening of electrostatic repulsions. Each micelle is characterized by an average aggregation number N_{ag} of about 70, and the fraction of C12 which participate to the formation of clusters is well correlated to the value previously found with ^{13}C NMR experiments. The data obtained from the solution are more difficult to fit because of the very weak scattering intensity, but nevertheless the parameters obtained for a 6% solution (see Table 4) are realistic and consistent with the aggregation behavior obtained from ^{13}C NMR.

Once again, this comparison between sol and gel confirms the significant increase in the degree of organization of the transient network during the gel formation as well as the increase of the clustering state of hydrophobic tails with increasing polymer concentration.

Network Architecture of the Gels. Although ideally each dithiol should form an intermolecular bridge between two different PAA chains, there are other possibilities which will affect the architecture and the properties of the network: intramolecular formation of a loop and dangling chains with a thiol end group. Furthermore, some dithiols molecules dissolved in water could remain fully unreacted. All these possibilities are schematically shown in Figure 14. At high polymer concentration ($C = 10\%$) the different titration methods indicate that the concentration of double bonds in the precursor is [C=C] $= 1.1 \times 10^{-4}$ mol/L, while the initial concentration of thiol functions is [SH] $= 9 \times 10^{-5}$ mol/L. This result is consistent with the under stoichiometry concentration of thiols inferred from the rheological measurements carried out close to the percolation threshold ($G' \sim G'' \sim \omega^{0.85}$).

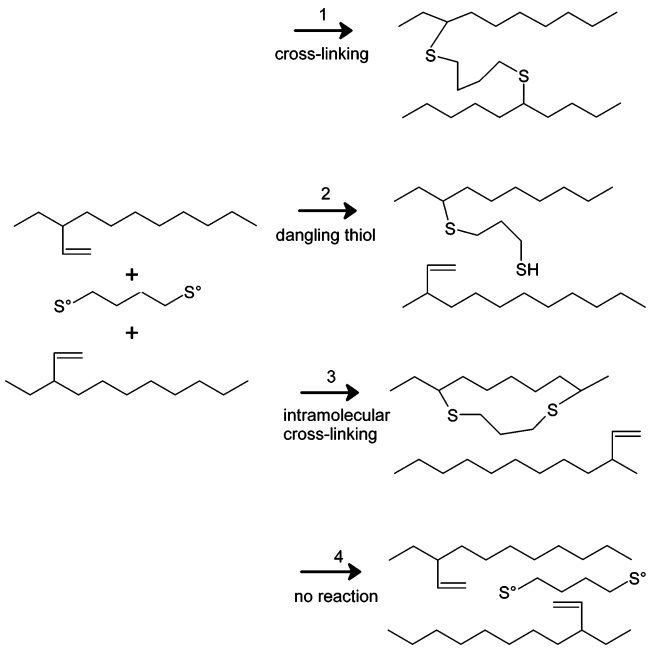

Figure 14. Schematic representation of the competition between all possible reactions during gelation. Reaction 1 only allows gelation.

Moreover, less than 2% of free thiols are found in the extracted water, indicating that the situation 4 in Figure 14 is almost nonexistent. After gelation, 35% of the initial double bonds and 20% of the initial thiols remain reactive in the system (dithiols which are grafted to the PAA chains by only one side). The consistency between the two titration methods also demonstrates that the thiol−thiol reaction giving disulfur bonds is negligible during the time of the gelation process, as observed by Nouiri et al.[46] We can conclude that 40% of the thiol functions are creating dangling thiols (case 2 in Figure 14), while 60% are involved in inter- and intramolecular cross-linking. Identical ratios were found in the entangled regime for a 6% PAA hydrogel and for a 6% PAA3C12 hydrogel, in agreement with the hypothesis that the network formation is not influenced by the presence of hydrophobic clusters in the gel. For gelation experiments carried out at lower concentration ($C < 6\%$), in the unentangled regime, titration and calorimetry (see Figures 4 and 5) clearly indicate a lower conversion of the thiol−ene reaction. At $C = 5\%$, for example, 10% of SH functions are found in the extracted water and 70% form dangling chains (attached by one end), so that only 20% of thiol functions are effectively involved in intra- or interchain bonding. In the unentangled regime the probability of cross-linking and the extent of the reaction both appear to decrease rapidly. The structures of hydrogels, obtained at various concentrations in the entangled and unentangled regimes, are summarized in Table 5 and Figure 15.

Mechanical Characterization of Hydrogels. Another way to probe the network structure is the measurement of the elastic modulus. According to Obukhov et al.,[47] the small strain shear modulus of an unentangled network in the linear regime is

Table 5. Structure of Hydrogels According to Their Concentration

C	5%	≥ 6%
intra or inter −S (2 and 3)	20%	60%
free −SH (1)	10%	< 2%
dangling −SH (4 and 4′)	70%	40%

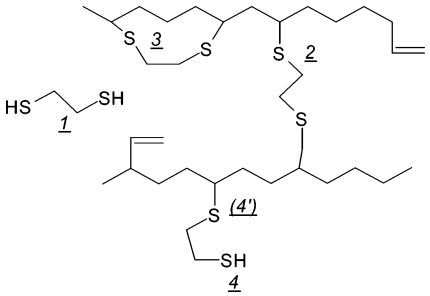

Figure 15. Schematic representation of the hydrogels with each possible function.

simply proportional to the density of elastically active strands and should be corrected by the effects due to differences (in terms of polymer and charge concentration) between the preparation state and the measurement state. In all generality, the shear modulus can be written as

$$G = A\frac{CRT}{M_{cth}}\left(\frac{\phi_i}{\phi}\right)^{2/3}\left(\frac{R_i}{R_0}\right)^2 \quad (7)$$

where A is a prefactor depending on the model chosen ($1 - 2/f$ for the phantom network or 1 for the Flory network), C is the concentration of polymer in the sample, M_{cth} is the average molecular weight between cross-link points, ϕ_i and ϕ are the polymer volume fractions in the preparation state and in the measurement state, respectively, R_i is the root-mean-square end-to-end distance of a network strand in the preparation state, and R_0 is the end-to-end distance the strand would have if it were a free chain of the same number of monomers in solution at a polymer and charge concentration equivalent to the measurement state. In our case the preparation state and the measurement state are identical in both polymer and charge concentration, and consequently we can estimate that $R_i \sim R_0$. Hence, eq 7 simplifies to

$$G_{0,affine} = \frac{CRT}{M_{cth}} \quad (8)$$

Of course, in highly swollen charged networks, chains can be stretched to the point were elasticity is no longer Gaussian and the finite extensibility of the chain can be felt. However, in the range of concentration we used—5 to 10% w/w—we are sufficiently far from the equilibrium swelling ($C \sim 1\%$; see Table 3) to neglect the non-Gaussian elasticity phenomena.[48]

If we assume finally that all double bonds form a bridge between two chains, that chain ends of the PAA chains can be neglected, and that the dithiol is sufficiently short not to contribute to the elasticity, each reacted double bond corresponds to an elastic chain, and the modulus is simply given by the number of double bonds per unit volume in the gel.

For a concentration of 100 kg/m^3 (as PAA is dissolved at 10% in water) and a theoretical M_{cth} of 0.94 kg/mol (one cross-link each 10 monomers, with a molar mass of 0.094 kg/mol for a monomer) if we assume that the reaction is complete and stoichimetric, we found a theoretical $G_{0,affine} \sim 260$ kPa.

Using the model of the phantom network, which takes into account the fluctuation of the network points, the shear modulus of a sample is given by

$$G_{0,phantom} = \frac{1}{2}\frac{CRT}{M_{cth}} \quad (9)$$

for a functionality of the network of 4.

If the cross-linker is assumed to be punctual compared to the chain length, f can be assumed to be equal to 4 and $G_{0,phantom} = G_{0,affine}/2 \sim 130$ kPa. Experimentally, we obtain a modulus $G' = 15$ kPa for a 10% PAA10db hydrogel, i.e., much lower than the two theoretical moduli calculated above. Hence, if all the thiol functions are attached to the PAA chain by at least one end and 60% by their two ends as shown by titration, only about 1 in 10 of them are effectively involved in the cross-linking of our sample, so the others (about 50%) are involved in intramolecular cross-linking.

For a 6% hydrogel, hydrophobically modified or not (see Figure 8), the rheology gives a modulus of 3 kPa, while, following the same theoretical approach, G_0 should be comprised between 150 and 75 kPa. Yet, as shown by the titration and the DSC results, 80% of the thiol−ene reaction occurs in these conditions. In consequence, it seems that there is, in proportion, more intramolecular cross-linking in the 6% sample than in the 10% one, which can be explained by dilution. As the PAA concentration decreases, the average distance between macromolecular chains increases, and the small dithiol cross-linker, once attached by one end to a chain, has less probability to react with another chain in its close vicinity. With these analyses, we can complete our previous data and give a more accurate picture of the networks from a point of view of the double bonds introduced into the macromolecular backbone (see Table 6).

As we can see, the proportion of initial double bonds which effectively gives rise to chemical cross-links is very low regardless of the concentration. As previously described, this can be attributed to the low concentration of reactive groups, coupled with the short size of the cross-linker and to its very low mobility (low diffusion constant) once attached by one side on the polymer chain.

Additional information can be obtained by comparing the rheological and DSC results, and we report in Figure 16 the variation of the dynamic moduli vs the conversion of the thiol−ene reaction determined at several concentrations.

These figures clearly show that the more concentrated the gel is, the faster the gel process occurs, although the kinetics of the thiol−ene reaction itself is not influenced by the concentration in the entangled regime. It confirms our hypothesis that, as dilution increases, the cross-linking probability decreases compared to the probability of forming intramolecular loops. Besides, we can remark that, for concentrated hydrogels (>8% w/w), the plateau value of the moduli are reached although the reaction is still far from ending. This can be explained by the fact that the rigidity of the macromolecular structure strongly increases during the network formation. Then, the probability for a short thiol, initially attached by one end to the PAA backbone, to bind another PAA chain is dramatically decreased at high conversion.

Rheological Properties of Hydrogels. The viscoelastic properties of hydrogels were studied after completion of the reaction ($f = 1$ Hz, $\gamma = 1\%$), and the dynamic moduli are reported as a function of concentration in Figure 17a,b.

All the systems investigated are predominantly elastic materials with a storage modulus G' much higher than the loss modulus G''. It seems quite clear that G' is mainly controlled by the chemical cross-links, as it is almost independent of the presence or absence of hydrophobic groups (see Figures 8 and 16b), while the loss modulus is mainly controlled by the hydrophobic

Table 6. General Structure of Hydrogels at Various Concentrations

C	5%	6%	8%	10%
$G_{0,\text{phantom}}$ (kPa)	65	75	100	130
G'_{exp} (kPa)	0.85	3	7	15
free C═C	65%	35%	35%	35%
inter −C−S−R−S−C− (2 in Figure 14)	<2%	4%	7%	12%
intra −C−S−R−S−C− (3)	7%	46%	43%	38%
dangling −CS−R−SH (4 and 4′)	28%	15%	15%	15%

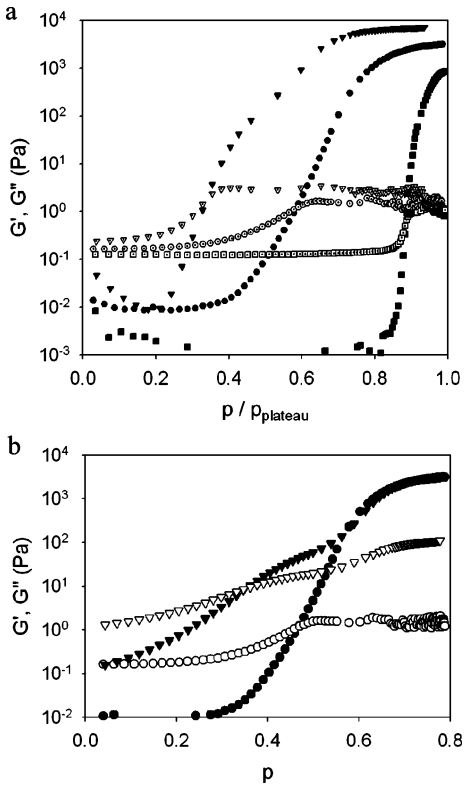

Figure 16. (a) Variation of dynamic moduli vs conversion for a PAA10db hydrogel at 8% (▼, G'; ▽, G''), 6% (●, G'; ○, G''), and 5% (■, G'; □, G''). (b) Comparison of the gelation process between a PAA3C12 (▼, G'; ▽, G'') and a PAA10db hydrogel (●, G'; ○, G'') at 6%.

associations. If we examine these results in more detail, it appears that the concentration dependence of G' is different in the entangled regime ($G' \sim C^{3.2}$ for gel concentrations higher than 6%) and in the unentangled one ($G' \sim C^5$ for hydrophilic gel below 5%). Surprisingly, the modified hydrogels still follow the C^3 dependence at lower concentrations (up to 4% for the 3C12 and 3% for the 5C12), and this can be explained if we consider that hydrophobic groups, forming physical cross-links, effectively contribute to the shear modulus of the sample. We believe that the sharp concentration dependence of the elastic modulus is partly due to the synthesis pathway which favors the formation of chemical cross-links with increasing concentration. In Figure 18, the storage modulus has been plotted as a function of the relative distance to the gel point (or reduced concentration):

$$\epsilon = (C - C_g)/C_g \qquad (10)$$

where C is the gel concentration and C_g the critical concentration at the gel point. The same reference has been used for all the systems: $C_g = 2\%$.

As we can see, the whole set of data can be fitted by the same power law $G \sim \epsilon^z$, with $z \cong 2.6$ for all the gels (2.5, 2.6, and 2.8 were found respectively for PAA, PAA3C12, and

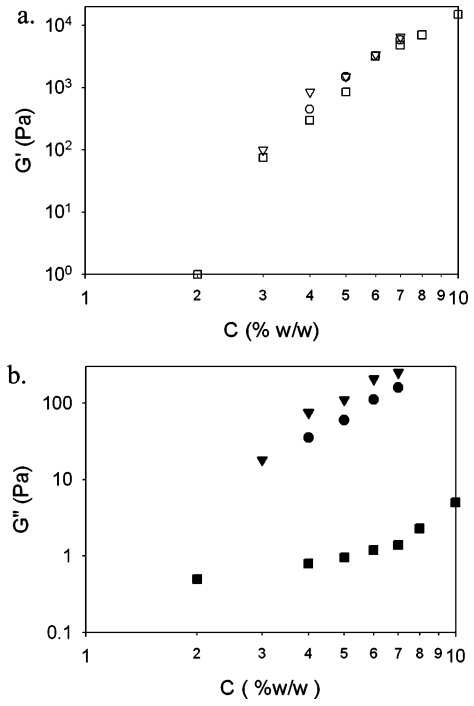

Figure 17. Evolution of G' (a: hollow symbols) and G'' (b: filled symbols) with the concentration for various hydrogels: PAA10db (□, ■), PAA3C12 (○, ●), and PAA5C12 (▽, ▼).

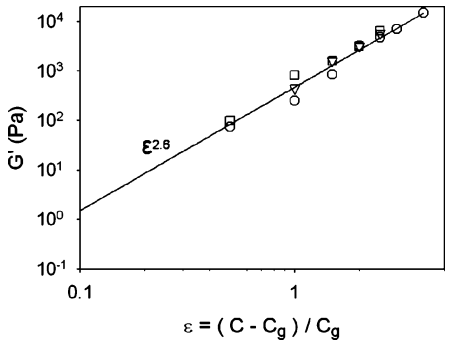

Figure 18. Variation of the storage modulus G' vs reduced concentration ϵ.

PAA5C12). Different theories have been developed to describe the power law dependence of the plateau modulus.

According to Rubinstein et al.,[49] three different regimes are expected depending on the gel state: (i) critical percolation with $z \sim 2.6$, (ii) mean-field unentangled regime with $z = 3$, and (iii) mean-field entangled regime with $z = 14/3$. In the present case, our results are in good agreement with the critical percolation regime proposed by Rubinstein et al.[49] or with the theoretical prediction of Martin et al.[50,51] based on the percolation theory ($z = 8/3$), for either the Rouse behavior (without considering hydrodynamic interactions) or the Zimm one (hydrodynamic interactions are taken into account). In the critical percolation regime,[49] permanent entanglements in the gel are not expected to be important. From a general point of view, the large variation of the experimental scaling exponent z (z values are usually obtained between 1.9 and 3.5) with the nature of the gels studied strongly suggests that z is deeply related to the chemical structure of the gel, both chemical[52,53] and physical,[54,55] and to their conditions of formation.

Coming back to Figure 17, one of the most spectacular feature of these hydrogels is the large increase of G'' with the hydrophobic content. Comparing the hydrophilic gel PAA10db with PAA3C12, the loss modulus is increased by ~2 decades.

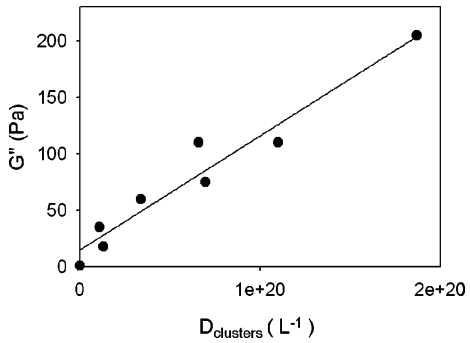

Figure 19. Evolution of the loss modulus with the density of clusters.

The effect is even more important for the PAA5C12 hydrogels, as $G''_{5C12} \sim 2G''_{3C12}$. The role played by the associating clusters of hydrophobic side groups to create dissipative processes is one the most interesting results of this study. Since the size of the clusters does not appear to change much with concentration of hydrophobic groups, the main parameter should be the density of clusters per unit volume, and we represent in Figure 19 the loss modulus G'' for a series of gels with increasing density of clusters. The density of clusters was estimated as follows:

$$D_{\text{clusters}} = \frac{C_{\text{PAAxC12}}\rho\tau_{\text{C12}}f_{\text{C12}}N_{\text{AV}}}{M_{\text{PAAxC12}}N_{\text{Ag}}} \qquad (11)$$

where C_{PAAxC12} is the polymer concentration in the gel, ρ is the water density, τ_{C12} is the fraction of C12 in the modified polymer, f_{C12} is the fraction of C12 which participate to the aggregation, N_{AV} is the Avogadro number, M_{PAAxC12} is the molar mass of the modified polymer, and N_{ag} is the aggregation number or number of C12 per micelle. D_{clusters} was calculated for PAA3C12 and PAA5C12 at 4, 5, and 6%, using the ^{13}C NMR and SANS results.

It is remarkable that the loss modulus appears to increase linearly with the density of clusters as if no interactions were present between clusters. From Figure 19, we can obtain a typical dissipative energy per aggregate

$$E_{\text{d}} \sim 10^{-21}\ \text{J} \sim {}^1/_4 k_{\text{b}}T$$

where k_{b} is the Boltzmann constant and T the room temperature. This energy is not negligible, as for example, in a rubber; the energy of an elastic segment is roughly $k_{\text{b}}T$.

The frequency dependence of the plateau moduli was finally studied for both unmodified and hydrophobically modified hydrogels (see Figure 20): when the reaction is completed, a frequency sweep from 0.1 to 20 Hz was carried out for each gel and for various concentrations. Although all gels were predominantly elastic, unmodified PAA behaves in a nearly perfect elastic way in the range of frequencies investigated (less than 2% variations on G' between 0.1 and 20 Hz, no significant variations on G'' as it stays extremely low compared to the G'). On the other hand, the hydrophobically modified PAA shows a real dependence with frequency (20% on the G' value in 2 decades of frequencies, almost 100% on the G'' value). It is noteworthy to point out that these differences in viscoelastic properties occur for nearly identical values of storage modulus and that they appear clearly in the linear regime of deformation, i.e., in the steady state.

The initial goal of the study was to synthesize in a controlled way hydrogels displaying both a low elastic modulus and dissipative properties which could have made the gels tougher. On the basis of the results presented in Figure 20, it is clear

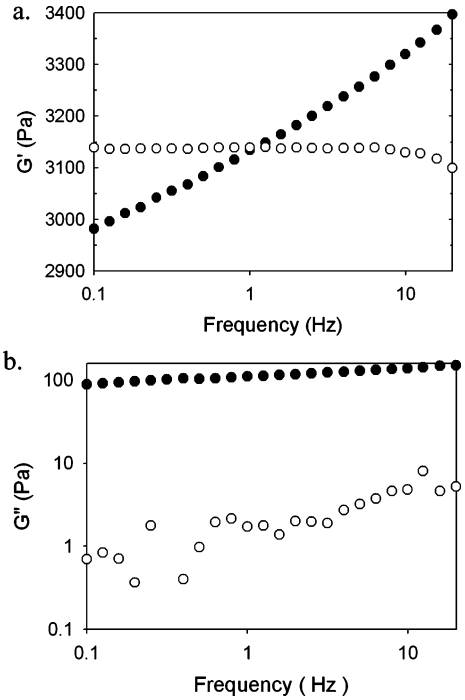

Figure 20. Comparison of G' (a) and G'' (b) for PAA (white symbols) and PAA3C12 (black) gels at $C = 6\%$ during a frequency sweep.

that the first two goals have been achieved: the introduction of hydrophobic groups along the backbone of the main chain is a very versatile tool to introduce a controlled degree of viscoelasticity in the material. Despite a much better ordered structure in the gel than in the solution (from SANS data), dissipative mechanisms are present at small strains, in a situation where it is difficult to see a mechanical breakdown of the clusters. It is likely that the number of carbons of the hydrophobic side group as well as the distance between side groups will play a role in these dissipative mechanisms.

Conclusion

We synthesized and characterized new hydrophobically modified PAA hydrogels, displaying the elastic behavior expected from a classical gel but with a much larger loss modulus.

The hydrophobic groups self-assembled to form micelles within the gel, and these micelles displayed a much better long range order than their un-cross-linked precursors in aqueous solutions as shown by NMR and SANS measurements.

Both DSC and rheological measurements showed that the kinetics of the chemical gelation process was not perturbed by the presence of the hydrophobic groups. Two characteristic transitions times, related respectively to the hydrophobic groups (t_1) and to the chemical cross-linking (t_2), were clearly apparent in the rheological measurement. While t_1 was directly related to the density of hydrophobic groups, t_2 was independent of it and depended only on the concentration of polymer in the solution. In terms of gel architecture, we observed a sharp difference, in the network of cross-links between two regimes of polymer concentration, corresponding to the unentangled and entangled regime of the respective PAA solutions.

A most significant result of our study is the synthesis of a series of hydrogels with identical elastic moduli but variable loss moduli. Such a class of hydrogels is expected to be interesting for applications where a controlled degree of viscoelasticity is necessary.

Furthermore, we expect these modified gels to display significantly different properties in large strain and fracture because of dissipative mechanisms induced by the hydrophobic micelles. Such investigations are currently in progress and will be reported in forthcoming papers.

Acknowledgment. We thank Guylaine Ducouret (Laboratoire PPMD, ESPCI) and Madeleine Djabourov (Laboratoire PMMH, ESPCI) for helpful conversations and technical advice on performing rheological measurements on gels and interpreting them. We also thank Annie Brûlet (LLB, CEA) for the SANS experiments.

References and Notes

(1) Volpert, E.; Selb, J.; Candau, F. *Macromolecules* **1996**, *29*, 1452.
(2) Volpert, E.; Selb, J.; Candau, F. *Polymer* **1998**, *39*, 1025.
(3) Durmaz, S.; Okay, O. *Polymer* **2000**, *41*, 3693.
(4) Cicek, H.; Tuncel, A. *J. Polym. Sci., Part A* **1998**, *36*, 527.
(5) Skouri, R.; Schosseler, F.; Munch, J. P.; Candau, S. J. *Macromolecules* **1995**, *28*, 197.
(6) Jabbari, E.; Nozari, S. *Eur. Polym. J.* **2000**, *36*, 2685.
(7) Okay, O.; Sariisik, S. B.; Zor, S. D. *J. Appl. Polym. Sci.* **1998**, *70*, 567.
(8) Breedveld, V.; Nowak, A. P.; Sato, J.; Deming, T. J.; Pine, D. J. *Macromomecules* **2004**, *37*, 3943.
(9) Muniz, E. C.; Geuskens, G. *Macromolecules* **2001**, *34*, 4480.
(10) Orkay, O.; Durmaz, S. *Polymer* **2002**, *43*, 1215.
(11) Van den Bulcke, A. I.; Bogdanov, B.; De Rooze, N.; Schacht, E. H.; Cornelissen, M.; Berghmans, H. *Biomacromolecules* **2000**, *1*, 31.
(12) Lee, J.; Macosko, C. W.; Urry, D. W. *Macromolecules* **2001**, *34*, 5968.
(13) Kong, H.-J.; Lee, K. Y.; Mooney, D. J. *Polymer* **2002**, *43*, 6239.
(14) Kong, H.-J.; Wong, E.; Mooney, D. J. *Macromolecules* **2003**, *36*, 4582.
(15) Gong, J. P.; Katsuyama, Y.; Kurokawa, T.; Osada, Y. *Adv. Mater.* **2003**, *15*, 1153.
(16) Medalia, A. *Rubber Chem. Technol.* **1978**, *51*, 437−523.
(17) Rigbi, Z. *Adv. Polym. Sci.* **1980**, *36*, 21.
(18) Shalaby, S.; McCormick, C.; Butler, G. G. *Water Soluble Polymers, Synthesis, Solution Properties and Applications*; *ACS Symp. Ser.* **1991**, *No. 467*.
(19) Iliopoulos, I.; Wang, T. K.; Audebert, R. *Langmuir* **1991**, *7*, 617.
(20) Hill, A.; Candau, F.; Selb, J. *Prog. Colloid Polym. Sci.* **1991**, *84*, 61.
(21) Annable, T.; Buscall, R.; Ettelaie, R.; Whittlestone, D. J. *J. Rheol.* **1993**, *37*, 695.
(22) Yekta, B. X.; Duhamel, J.; Adiwidjaja, H.; Winnik, M. A. *Macromolecules* **1995**, *28*, 956.
(23) Hoffman, A. S. *Adv. Drug Delivery Rev.* **2002**, *43*, 3.
(24) Clark, A. H.; Ross-Murphy, S. B. *Adv. Polym. Sci.* **1987**, *83*, 59.
(25) Dobrynin, A. V.; Colby, R. H.; Rubinstein, M. *Macromolecules* **1995**, *28*, 1859.
(26) Dobrynin, A. V.; Rubinstein, M. *Macromolecules* **2000**, *33*, 8097.
(27) Patrickios, C. S.; Georgiou, T. K. *Curr. Opin. Colloid Interface Sci.* **2003**, *8*, 76.
(28) Gholap, S. G.; Jog, J. P.; Badiger, M. V. *Polymer* **2004**, *45*, 5863.
(29) Cram, S. L.; Brown, H. M.; Spinks, G. M.; Creton, C.; Hourdet, D. *Macromolecules* **2005**, *38*, 2981.
(30) Magny, B.; Lafuma, F.; Iliopoulos, I. *Polymer* **1992**, *33*, 3151.
(31) Boileau, S.; Mazeaud-Henri, B.; Blackborow, R. *Eur. Polym. J.* **2003**, *39*, 1395.
(32) Romani, F.; Passaglia, E.; Aglietto, M.; Ruggeri, G. *Macromol. Chem. Phys.* **1999**, *200*, 524.
(33) Cramer, N. B.; Scott, J. P.; Bowman, C. N. *Macromolecules* **2002**, *35*, 5361.
(34) Schapman, F.; Courcevelle, J. P.; Bunel, C. *Polymer* **2000**, *41*, 17.
(35) Vogel, A. I. *A Textbook of Quantitative Inorganic Analysis Including Elementary Instrumental Analysis*, 3rd ed.; Longmans: New York, 1961.
(36) Cotton, J. P. In *Neutron, X-Ray and Light Scattering*; Lindner, P., Zemb, T., Eds.; Elsevier: North-Holland, 1991; p 1.
(37) Rubinstein, M.; Semenov, A. N. *Macromolecules* **2001**, *34*, 1058.
(38) Cramer, N. B.; Davies, T.; O'Brien, A. K.; Bowman, C. N. *Macromolecules* **2003**, *36*, 4631.
(39) Chambon, F.; Winter, H. H. *J. Rheol.* **1986**, *30*, 367.
(40) Chambon, F.; Winter, H. H. *J. Rheol.* **1987**, *31*, 683.
(41) Winter, H. H.; Mours, M. *Adv. Polym. Sci.* **1997**, *134*, 166.
(42) Petit-Agnely, F.; Iliopoulos, I. *J. Phys. Chem. B* **1999**, *103*, 4803.
(43) Philippova, O. E.; Hourdet, D.; Audebert, R.; Kholkhov, A. R. *Macromolecules* **1997**, *30*, 8278.
(44) Barbier, V.; Hervé, M.; Sudor, J.; Brulet, A.; Hourdet, D.; Viovy, J. L. *Macromolecules* **2004**, *37*, 5682.
(45) Hourdet, D.; Gadgil, J.; Podhajecka, K.; Badiger, M. V.; Brulet, A.; Wadgaonkar, P. P. *Macromolecules* **2005**, *38*, 8512.
(46) Nouiri, M. Thesis, University of Montpellier, 1990.
(47) Obukhov, S. P.; Rubinstein, M.; Colby, R. H. *Macromolecules* **1994**, *27*, 3191.
(48) Nisato, G.; Skouri, R.; Schosseler, F.; Munch, J. P.; Candau, S. J. *Faraday Discuss.* **1995**, *101*, 133.
(49) Rubinstein, M.; Colby, R. H. *Macromolecules* **1994**, *27*, 3184.
(50) Martin, J. E.; Adolf, D.; Wilcoxon, J. P. *Phys. Rev. Lett.* **1988**, *61*, 2620.
(51) Martin, J. E.; Adolf, D. *Annu. Rev. Phys. Chem.* **1991**, *42*, 311.
(52) Koike, A.; Nemoto, N.; Watanabe, Y.; Osaki, K. *Polym. J.* **1996**, *28*, 942.
(53) Axelos, M. A. V.; Kolb, M. *Phys. Rev. Lett.* **1990**, *64*, 1457.
(54) Li, L.; Aoki, Y. *Macromolecules* **1998**, *31*, 740.
(55) Bromberg, L. *Macromolecules* **1998**, *31*, 6148.

MA061361N